DEVELOPMENT OF FOCUSING ALGORITHMS FOR ARC-SCANNING GROUND-BASED SYNTHETIC APERTURE RADAR

Hoonyol Lee[1], Seong-Jun Cho[2] and Kwang-Eun Kim[2]

[1]Department of Geophysics, Kangwon National University (hoonyol@kangwon.ac.kr)
[2]Korea Institute of Geosciences and Mineral Resources (mac@kigam.re.kr, kimke@kigam.re.kr)

ABSTRACT ... KIGAM and KNU are developing a ground-based Arc-scanning SAR system (ArcSAR) mounted on a truck. The system achieves the coherent integration of radar returns from ground targets by the circular motion of the antennae attached to the end of an extendable arm. Precise control of antenna position and the extended coherent-integration-length enable the formation of high-resolution, high-precision and phase-preserving SAR images. Based on the Polar Format Algorithm, two SAR-focusing algorithms were developed for the data acquired from two different scanning modes of this unique system: the scan mode and the spot mode. This paper presents the details of the ArcSAR focusing algorithms and the results tested on a simulated data and an acquired data.

KEY WORDS: ArcSAR, synthetic aperture radar, Polar Format Algorithm, scan mode, spot mode

1. INTRODUCTION

Ground-Based SAR (GB-SAR) systems have been actively developed recently not just as an alternative to satellite SAR systems but with its own merit of accuracy and repeatability for regional applications [1]-[12]. KIGAM and KNU are developing a new ground-based Arc-scanning Synthetic Aperture Radar (ArcSAR) system mounted on a truck. The ArcSAR system acquires images by transmitting and receiving microwave signals through the antennae attached to the end of the extendable boom. The boom is mounted on top of the platform that rotates by the circular rail guide. The RF part of the system is mainly composed of a vector network analyzer, microwave amplifier, microwave switch system, and a notebook computer. Any kind of antenna can be attached to the boom as long as its weight and shape do not harm the stability of the system.

A stepped-frequency microwave signal is generated from the vector network analyzer. The signal is sent to the selected polarization of the Tx antenna by the microwave switch system. The signal returned from the target is collected by the Rx antenna with a particular polarization selected by the switch system. The data are then stored to the hard disk of the notebook computer for the SAR focusing. The system has the different geometry from the conventional linear-scanning GB-SAR system and requires new focusing algorithms to produce images out of the scanned data.

The ArcSAR system can operates in two different scanning modes: the *spot* mode and the *scan* mode (Figure 1). In the spot mode, the antennae attached to the end of the boom can rotate in azimuth direction, enabling continuous look to the designated target area. The coherent integration arc is as long as the half-circle of the scanning boom to produce higher resolution than the conventional linear-scanning GB-SAR systems [1][2]. In the scan mode, the antennae are fixed relative to the boom during the scan. The data can be obtained continuously during the rotation so that it can image the whole azimuth angle (360°) around the system. The coherent integration arc is shorter than the spot mode producing lower resolution, but still has advantage in resolution when compared to the real aperture radar.

In this paper, we present the development of new focusing algorithms for the ArcSAR system. Based on the geometry similar to the Polar Format Algorithm and considering the processing costs, the Deramp-FFT algorithm is used for the spot mode while the Range-Doppler algorithm is used for the scan mode.

2. ALGORITHMS

2.1 ArcSAR Spot Mode Focusing: Deramp-FFT Algorithm in Polar Format

A point target $P(x_c, y_c)$ in rectangular coordinates can be expressed as $P(R_c, \theta_c)$ in polar coordinates as shown in Figure 2 and with the following relations

$$x_c = R_c \cos\theta_c, \; y_c = R_c \sin\theta_c . \quad (1)$$

The data is obtained in polar coordinates as the boom rotates. The data from this point target is base-banded and Hamming filtered in range direction. The data is inverse-FFTed in range direction to obtain a range compressed data,

$$s(\theta \mid R_c, \theta_c) = e^{-j\frac{4\pi}{\lambda}R(\theta|R_c,\theta_c)}, \quad |\theta - \theta_c| < \theta_s/2 = \pi/2, \quad (2)$$

where θ is the azimuth of the scan and θ_s is the *coherent integration arc*. The maximum θ_s is π for the spot mode. Given the length of the boom *r*, the range from the antenna to the target can be expressed as

$$R(\theta \mid R_c, \theta_c) = \sqrt{R_c^2 + r^2 - 2R_c \cos(\theta - \theta_c)} \quad (3)$$

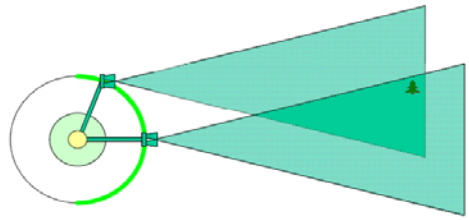

(a) Spot Mode

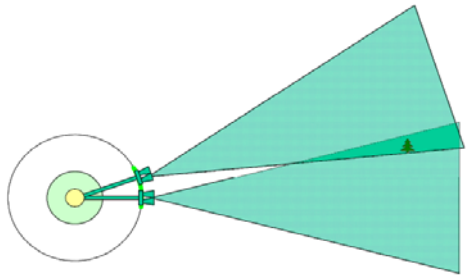

(b) Scan Mode

Figure 1. Two scanning modes of ArcSAR. The spot mode (a) produces high resolution image over the area overcastted by the antenna footprint due to the longer coherent-integration-arc (green arc), while the scan mode (b) can image 360° area around the system with low resolution but still higher than the conventional real-aperture radar system.

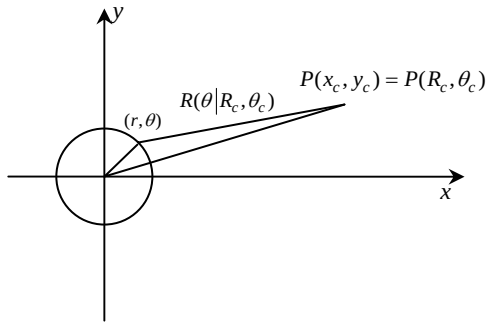

Figure 2. ArcSAR Geometry

Range migration is performed according to (3). The Taylor's expansion of (3) at $\theta = 0$ gives

$$R(\theta) = R(0) + R'(0)\theta + \frac{R''(0)}{2!}\theta^2 + \frac{R'''(0)}{3!}\theta^3 + \cdots \quad (4)$$

where,

$$R(0) = \sqrt{R_c^2 + r^2 - 2R_c r\cos\theta_c}\ , \quad (5)$$

$$R'(0) = -\frac{R_c r\sin\theta}{R(0)} = -\frac{ry_c}{R(0)}, \quad (6)$$

$$R''(0) = \frac{R_c r\cos\theta_c R(0) + R_c r\sin\theta_c R'(0)}{R^2(0)}. \quad (7)$$

The term higher than quadratic is ignored. The deramp function is then defined as

$$h^{-1}(\theta) = e^{j\frac{2\pi}{\lambda}R''(0)\theta^2} \quad (8)$$

with which the SAR focusing is performed by the following arc-matched filtering:

$$g(u) = \int s(\theta)h^{-1}(\theta)e^{-j2\pi u\theta}d\theta\,. \quad (9)$$

Here, the u is an arbitrary data space and the integration range over θ is $[\theta_c - \theta_s/2,\ \theta_c + \theta_s/2]$. The analytic evaluation of (9) gives the focused image:

$$g(u) = e^{-j\frac{4\pi}{\lambda}R_c}e^{-j2\pi\left(u-\frac{2r}{\lambda R_c}y_c\right)}\theta_s \mathrm{sinc}\left[\pi\theta_s\left(u - \frac{2r}{\lambda R_c}y_c\right)\right] \quad (10)$$

The above sinc equation has the maximum value at $u = 2ry_c/(\lambda R_c)$ and gives the definition of resolution as $\delta u = 1/\theta_s$ by the width of the half power of it. Therefore, the image for the point target is focused as the following relation

$$y_c = \frac{\lambda R_c}{2r}u\,, \quad (11)$$

with the azimuth resolution of

$$\delta y_c = \frac{\lambda R_c}{2r}\delta u = \frac{\lambda R_c}{2r\theta_s}\,. \quad (12)$$

The processed image is in (R_c, u) domain and should be geometrically transformed into (x, y) space using (1) and (11). One can expect higher resolution by enlarging the length of the antenna boom r, by increasing coherent integration arc θ_s, or by using higher center frequency λ. The resolution is a function of the range R_c as expected. For example, with r = 4 m, $\theta_s = \pi$, λ =0.031 m, we obtain the azimuth resolution

$$\delta y_c = 1.23\times10^{-3}R_c\,. \quad (13)$$

The resolution of a GB-SAR system with the linear scan-length of L_s is given as $\delta y_c = \frac{\lambda R_c}{2L_s}$ [2]. The arc scanning is equivalent to the linear scanning length of $L_s = \pi r$. This means that ArcSAR obtained the resolution of 12.5 m linear scan with the arc scan of 4 m antenna boom.

The phase of the focused image is $\phi = -4\pi R_c/\lambda$ so that the phase is preserved for the interferometric use as a function of range.

The Deramp-FFT algorithm simplifies the processing dramatically by making $R''(0)$ at a fixed θ_c to be the image center in the Deramp function. For example, we use $R''(0) = \frac{R_c r}{R_c - r}$ at $\theta_c = 0$ and irrespective of θ_c when the image center is parallel to the x direction. Therefore, the focused image is accurate only near the center of the image swath, and dispersed otherwise. Therefore the Deramp-FFT algorithm is suitable for the spot mode only where the image swath is narrow. Alternatively, we can construct the whole scan image obtained from the scan mode by mosaicking the Deramp-FFT results, but the algorithm for the scan mode can be optimized by the method described in the next section.

2.2 ArcSAR Scan Mode Focusing: Range-Doppler Algorithm in Polar Format

As the scan mode obtains data continuously in polar format for the target at $P(x_c, y_c)$ in rectangular coordinates or $P(R_c, \theta_c)$ in polar coordinates, the Range-Doppler algorithm in polar format is an efficient way of SAR focusing. After the range compression, the collected signal is represented as

$$s(\theta \mid R_c, \theta_c) = e^{-j\frac{4\pi}{\lambda}R(\theta|R_c,\theta_c)}, \quad |\theta - \theta_c| < \theta_s/2 = \frac{\lambda}{2L} \qquad (14)$$

where L is the size of the antenna in horizontal direction. The coherent integration arc for the scan mode is limited by the width of the antenna beam. Similarly, we have the range from the antenna to the target as

$$R(\theta \mid R_c, \theta_c) = \sqrt{R_c^2 + r^2 - 2R_c r\cos(\theta - \theta_c)}\,. \qquad (15)$$

Differently from the spot mode, we expand the above equation at the target itself, $\theta = \theta_c$ so that

$$R(\theta) = R(\theta_c) + R'(\theta_c)\theta + \frac{R''(\theta_c)}{2!}\theta^2 + \frac{R'''(\theta_c)}{3!}\theta^3 + \cdots \qquad (16)$$

where,

$$R(\theta_c) = R_c - r \qquad (17)$$

$$R'(\theta_c) = 0 \qquad (18)$$

$$R''(\theta_c) = \frac{R_c r}{R(\theta_c)} = \frac{R_c r}{R_c - r} \qquad (19)$$

Ignoring the terms higher than quadratic and by using the wavenumber Doppler parameters, we obtain

$$R(\theta) = R(\theta_c) - \frac{\lambda u_{Dc}}{2}(\theta - \theta_c) - \frac{\lambda u_R}{4}(\theta - \theta_c)^2 + \cdots \qquad (20)$$

with

$$\text{Doppler Centroid: } u_{Dc} = 0\,, \qquad (21)$$

$$\text{Doppler rate: } u_R = -\frac{2}{\lambda}\frac{R_c r}{R_c - r}\,, \qquad (22)$$

so that the received signal becomes

$$s(\theta \mid R_c, \theta_c) = e^{-j\frac{4\pi}{\lambda}R(\theta_c)} e^{j2\pi\left[u_{Dc}(\theta-\theta_c) + u_R(\theta-\theta_c)^2/2\right]}. \qquad (23)$$

The signal comprises a linear chirp as a function of azimuth. The matched filter for Range-Doppler algorithm is defined as

$$h^{-1}(\theta) = e^{-j2\pi\left[u_{Dc}\theta + u_R\theta^2/2\right]} \qquad (24)$$

The data is compressed in azimuth direction by the following filtering

$$g(\theta) = \int h^{-1}(\theta' - \theta)\, s(\theta')\, d\theta'\,. \qquad (25)$$

The evaluation of the above integration with the range of θ' to be $[\theta_c - \theta_s/2,\ \theta_c + \theta_s/2]$ gives

$$g(\theta) = e^{-j\frac{4\pi}{\lambda}(R_c - r)} e^{j2\pi\left[\frac{(\theta-\theta_c)^2}{\lambda(R_c - r)}\right]} \times \theta_s \mathrm{sinc}\left[\frac{2\pi R_c r\theta_s}{\lambda(R_c - r)}(\theta - \theta_c)\right] \qquad (26)$$

The above signal has a maximum value to be θ_s at $\theta = \theta_c$. The azimuth angular resolution is defined as

$$\delta\theta = \frac{\lambda(R_c - r)}{2R_c r\theta_s}\,. \qquad (27)$$

The phase is $\phi = -\frac{4\pi}{\lambda}(R_c - r)$ so that the image is from the antenna (not from the center of the arc) to the target. The processed image is in (R, θ) domain and should be transformed into (x, y) space for display using (1). The azimuth resolution in meter is then

$$\delta\theta R_c = \frac{L}{2r}(R_c - r)\,, \qquad (28)$$

which is again a function of R_c but is irrespective of wavelength λ. For the X-band system as an example, with r = 4 m, L =0.15 m,

$$\delta\theta R_c = 1.88\times10^{-2}(R_c - r)\,. \qquad (29)$$

The resolution of the scan mode is 15 times poorer than the spot mode in (13), but is 11 times better than that of the real aperture radar given by

$$\delta\theta R_c = \frac{\lambda}{L}R_c = 2.07\times10^{-1}R_c\,. \qquad (30)$$

3. COMPARISION OF RESOLUTIONS

The resolutions and their ratios from the various ground-based radar systems are listed in Table 1. Azimuth angular resolutions (in radian) and their ratios are depicted as formulae in the lower half triangle of the table, while ratios of X-band system are in the upper half triangle as an example.

The X-band system has the wavelength of λ =0.031 m, the azimuth antenna width of L =0.15 m, the length of the boom r =4 m, the coherent integration arc of $\theta_s = \pi$ for the ArcSAR Spot Mode, and the linear scanning GBSAR length of L_s =4 m (the same as the boom) for comparison.

As expected, Arc-scanning Real Aperture Radar (ArcRAR) will have the poorest resolution because the azimuth resolution is simply the beam width of the antenna.

The resolution of the ArcSAR Scan Mode will be enhanced by 11 times over the ArcRAR. ArcSAR Scan Mode is 4.8 times and 15.2 times lower than linear GB-SAR or ArcSAR spot mode but has the advantage of omnidirectional coverage.

ArcSAR Spot Mode will have the resolution 3.1 times higher than the linear-scanning GB-SAR system when compared with the equal length of the rotational boom and linear scanning length of 4 m. By scanning in arc rather than linear, ArcSAR spot mode will have the resolution equivalent to $L_s = \pi r$ linear scan. ArcSAR Spot Mode has 15.2 times higher resolution than ArcSAR Scan Mode, and 167.2 times over ArcRAR.

Table 1. Azimuth angular resolutions and their ratios between ArcRAR, ArcSAR Scan Mode, Linear-scanning GBSAR and ArcSAR Spot Mode. Numerical values are the ratio of resolutions based on an X-band system with L =0.15 m, r =4 m, L_s =4 m, $\theta_s = \pi$, and λ =0.031 m. The numbers in the parenthesis are the inverse of it.

Azimuth Resolution		ArcRAR	ArcSAR Scan	Linear GBSAR	ArcSAR Spot
ArcRAR	$\frac{\lambda}{L}$	1	9.07e-2 (11.0)	1.87e-2 (53.4)	5.98e-3 (167.2)
ArcSAR Scan	$\frac{L}{2r}$	$\frac{L^2}{2\lambda r}$	1	2.07e-1 (4.8)	6.58e-2 (15.2)
Linear GBSAR	$\frac{\lambda}{2L_s}$	$\frac{L}{2L_s}$	$\frac{\lambda r}{LL_s}$	1	3.18e-1 (3.1)
ArcSAR Spot	$\frac{\lambda}{2r\theta_s}$	$\frac{L}{2r\theta_s}$	$\frac{\lambda}{\theta_s L}$	$\frac{L_s}{r\theta_s}$	1

4. CONCLUSIONS

Image focusing algorithms for ArcSAR were developed in polar coordinates. The Deramp-FFT algorithm was used for ArcSAR Spot Mode and the Range-Doppler algorithm for ArcSAR Scan Mode. Comparisons of image resolutions between various ground-based radar systems confirmed the advantage of ArcSAR Scan Mode and ArcSAR Spot Mode over ArcRAR and Linear-scanning GBSAR. ArcSAR Spot Mode has the equivalent linear scan length of π times the radius and 167 times higher resolution than ArcRAR. ArcSAR Scan Mode has omnidirectional coverage with 11 times higher resolution than that of ArcRAR. The system will be mounted on a truck and will provide a rapid response tool for various applications such as regional mapping and environmental hazard monitoring.

ACKNOWLEDGEMENT

This research was supported by a grant (07KLSGC03) from Cutting-edge Urban Development - Korean Land Spatialization Research Project funded by Ministry of Land, transport and Maritime Affairs of Korean government.

REFERENCES

[1] Lee, H., Cho, S. J., Sung N. H., and Kim, J. H., 2007a. Development of a GB-SAR (I): System configuration and interferometry, *Korean Journal of Remote Sensing.*, 23(4), pp. 237-245.

[2] Lee, H., Cho, S. J., Sung N. H., and Kim, J. H., 2007b. Development of a GB-SAR (Ⅱ): Focusing algorithmⅡ, *Korean Journal of Remote Sensing.*, 23(4), pp. 247-256.

[3] Leva, D., Nico, G., Tarchi, D., Fortuny-Guasch, J., and Sieber. A. J., 2003. Temporal analysis of a landslide by means of a ground-based SAR interferometer, *IEEE Transactions on Geoscience and Remote Sensing*, 41(4), pp. 745-757.

[4] Luzi, G., Pieraccini, M., Mecatti, D., Noferini, L., Guidi, G. Moia, F. and Atzeni, C., 2004. Ground-Based Radar interferometry for landslides monitoring: Atmospheric and Instrumental decorrelation Sources on Experimental Data. *IEEE Transactions on Geoscience Remote Sensing*, 42(11), pp. 2454-2466

[5] Martinez-Vazquez, A., Fortuny-Guasch, J. and Gruber, U. 2005. Monitoring of the snow cover with a ground-based Synthetic Aperture Radar. *EARSel eProceedings*, 4. pp. 171-178

[6] Nico, G., Leva, D., Antonello, G., and Tarchi, D., 2004. Ground-based SAR interferometry for terrain mapping:
Theory and sensitivity analysis, *IEEE Transacations on Geoscience and Remote Sensing*, 42(6), pp. 1344-1350.

[7] Nico, G., Leva, D., Fortuny-Guasch, J., Antonello, G. and Tarchi, D., 2005. Generation of digital terrain models with a Ground-Based SAR system, *IEEE Transactions on Geoscience and Remote Sensing*, 43(1), pp. 45-49.

[8] Noferini L., Pieraccini, M., Mecatti, D., Luzi, G., Atzeni, A. C. and Broccolato, M., 2005. Permanent Scatterers Analysis for Atmospheric Correction in Ground-Based SAR Interferometry, *IEEE Transactions on Geoscience and Remote Sensing*, 43(7), pp. 1459-1471

[9] Pipia, L., Fabregas, X., Aguasca, A.. and Lopez-Martinez, C. 2008. Atmospheric artifact compensation in Ground-Based DInSAR application, *IEEE Geoscience and Remote Sensing Letters*, 5(1), pp. 88-92

[10] Tarchi, D., Casagli, N., Fanti, R., Leva, D., Luzi, G., Pasuto, A., Pieraccini, M. and Silvano, S. 2003. Landslide monitoring by using ground-based SAR interferometry: an example of application to the Tessina landslide in Italy, *Engineering Geology*, 68, pp. 15-30.

[11] Tarchi, D., Rudolf, H., Pieraccini, M. and Atzeni, C.. 2000. Remote monitoring of buildings using a ground-based SAR: application to cultural heritage survey, *International Journal of Remote Sensing*, 21(18), pp. 3545-3551.

[12] Zhou, Z. S., Boerner, W. M., and Sato, M. 2004. Development of a ground-based polarimetric broadband SAR system for noninvasive ground-truth validation in vegetation monitoring. *IEEE Transactions on Geoscience Remote Sensing.*, 42(9), pp. 1803-1810.